DESIGN OF REAL-TIME MONITORING SYSTEM FOR POWER DEVICE STATUS BASED ON OPTICAL FIBER SENSOR NETWORK

Jing LI[1], Xutao LU[2*], Shubo ZHAO [3], Yifeng REN[4]

In order to improve the state monitoring capability of power devices and simultaneously obtain temperature and dynamic and static stress responses, a state monitoring system was designed based on optical fiber sensor network. The chirped grating modulation technique was used on the Fiber Bragg Grating sensor package to make the temperature and strain response of the test position different, so that the simultaneous solution of the two parameters was realized by the decoupling algorithm. On the basis of constructing a two-parameter decoupling model, the trends of temperature and strain with respect to wavelength were simulated and analyzed. In the experiment, the state of the power device was tested and analyzed from three aspects. In the temperature calibration experiment, the temperature responds linearity reached 0.9986, and the deviation of the comparison test result with the FOT2300 temperature detector was better than 1.3%. In the static strain response experiment, the system sensitivity in the range of 0.1kN-1kN was 0.0036nm/N, and the system sensitivity in the range of 1kN-5kN was 0.0018nm/N. In the dynamic response experiment, the impact of heavy objects at different heights had obvious peak differences. The wavelength offset was inversely proportional to the time half-width, and the spectral line shape had obvious characteristics. It can be seen that the system has good distinguishability when obtaining the state information of power device temperature and static and dynamic stress.

Keywords: optical fiber sensor network; power device; two-parameter decoupling; temperature compensation; static and dynamic strain

1. Introduction

Optical fiber sensing online monitoring technology has the advantages of anti-electromagnetic interference, long life, small size, high sensitivity, and easy multiplexing [1-3]. Optical fiber composite ground wire technology also provides great convenience for the application of optical fiber in power transmission. At home and abroad, a large number of research works on the online monitoring of

[1] A. Prof., School of Electrical and Control Engineering, North University of China, China, e-mail: lj@nuc.edu.cn

[2] A. Prof., College of Mechatronics Engineering, North University of China, China, e-mail: luxutao@nuc.edu.cn **(Corresponding Author)**

[3] Engineer, Avic Changcheng Metrology &Measurement (Tian jin) Co., ltd Chongqing Branch, China, e-mail: zhaoshubo@zhccjl.com.cn

[4] Prof., School of Electrical and Control Engineering, North University of China, China, e-mail: renyifeng126@126.com

power equipment status by optical fiber sensing has been carried out, and there have been records of hanging network operation. At present, the monitoring of power equipment is no longer limited to the monitoring of voltage and current. Real-time monitoring of temperature and stress changes of power equipment has become an important means to analyze the safe operation of the system. For example, substation equipment, mine electrical equipment and so on all use temperature monitoring to avoid overheating risk. Traditional testing methods include digital temperature sensor, etc., but because these traditional sensors are electrically driven, there are certain risks, and the passive characteristics of optical fiber sensor can solve this problem well.

In terms of temperature monitoring, obtaining the operating status of power equipment by monitoring the temperature information of power equipment is a research hotspot of on-line monitoring of power systems [4]. The temperature measurement methods are divided into point temperature monitoring and distributed temperature monitoring. Point temperature monitoring includes fiber grating temperature monitoring and fluorescent fiber temperature monitoring, which are mainly used to monitor key abnormal parts in power equipment. Distributed temperature monitoring refers to monitoring using the above-mentioned scattering-type distributed optical fiber sensors, which is mainly used for omnidirectional measurement of transmission line temperature. HAMMON inserted the FBG (FBG, fiber Bragg grating) [5] temperature sensor into a sheath made of PTFE (Poly tetra fluoroethylene) and placed the sheath in the through hole of the transformer winding and the tank wall so that the sensor was not disturbed by strain, and the winding was realized. YI Jiang designed a special cross-probe package structure [6] to fix the sensor without glue, which improved the accuracy of online monitoring. WICKERSHEIM used a fluorescent optical fiber thermometer [7] to monitor the transformer winding, and the phosphorescent material probe was inserted into the transformer to detect the temperature through the relationship between the fluorescence intensity ratio and the temperature. ZHAO Yong designed and developed a small doped optical fiber temperature sensor [8] with a probe diameter of 1.8 mm and a temperature measurement accuracy of 0.45 ℃ in the range of 0-90 ℃. ZHAO Yongtan proposed a micro-nano optical fiber temperature sensor[9] with a probe diameter of only 2μm, which further realizes the interference-free measurement of the fine structure of the fluorescence lifetime optical fiber temperature sensor in the field of power equipment, but its temperature detection accuracy is not high, can only reach ±2℃[10]. It used a BOTDR (Brillouin optical time-domain reflectometer) with a temperature sensitivity of 1 ℃ as a distributed temperature sensor for monitoring, which is suitable for monitoring key parts of power equipment.

In terms of strain monitoring, the strain of the optical fiber can cause the wavelength of the optical fiber to change. By converting the measurement of

certain optical fiber parameters into the monitoring of the strain of the power equipment, it is possible to judge whether the equipment is working normally under the running state. According to the different principles of optical fiber strain sensing, strain monitoring methods are divided into fiber grating strain monitoring and scattering distributed strain monitoring. ZHAO Long used fiber grating to form a strain sensor [11], which was welded to the tower through a steel substrate to measure the strain of the tower. MA Guoming proposed a package structure with a flange [12], which solved the hysteresis problem of the tension sensor to a certain extent. WYDRA used a chirped fiber Bragg grating sensor to measure the sag of aluminum wire [13]. The sensor was directly installed in the middle of the wire, and its spectrum was about 10 times that of ordinary FBG, which greatly improved the sensitivity and accuracy of strain monitoring.

This paper mainly studies the real-time monitoring technology and application of temperature and strain of power devices based on optical fiber sensing network. An optical fiber sensor network applied to power structure is built, and the simultaneous demodulation of temperature and static and dynamic stress is realized by improving the packaging design of the FBG sensor.

2. Optical Fiber Sensor Network System

The monitoring of the state of the power device is mainly the real-time monitoring of the static and dynamic pressure and temperature field of the structure. In this paper, a new type of FBG deformation sensor is designed to cooperate with the temperature sensor to achieve dual-parameter decoupling. The strain sensing part is inserted into the top and bottom of the transformer winding structure, and it can be placed at the position where the outer winding of the transformer meets the outer structure for easy installation. In the temperature sensing part, a steel packaged FBG sensor is arranged in the same position, and temperature information is obtained at the same time. The system structure is shown in Fig. 1.

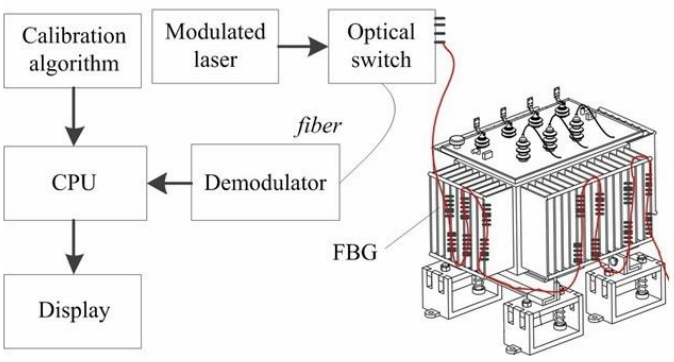

Fig.1 Power device condition monitoring system based on optical fiber sensor network

Since the demodulation system can complete the data acquisition of multiple FBGs at the same time, and the loss of the optical fiber in the transmission distance of several kilometers is negligible, the state monitoring of a large number of transformers in the entire substation can be completed through a demodulation system. When the number of FBGs on the same optical fiber is limited by the bandwidth, a large amount of FBG sensor data can be acquired by using a 1×N-type multiplex optical switch to complete time-sharing scanning.

3. Two-Parameter Decoupling Model

There is cross sensitivity between strain and temperature [14], but from the external structure design of the novel FBG probe, it can be seen that when the temperature changes, the response of the conical section and the cylindrical section is consistent, but for strain, the sensitivity of the conical section and the cylindrical section is Significantly different because h is included in the strain itself parameter. The packaging structure of the novel FBG probe is shown in Figure 2.

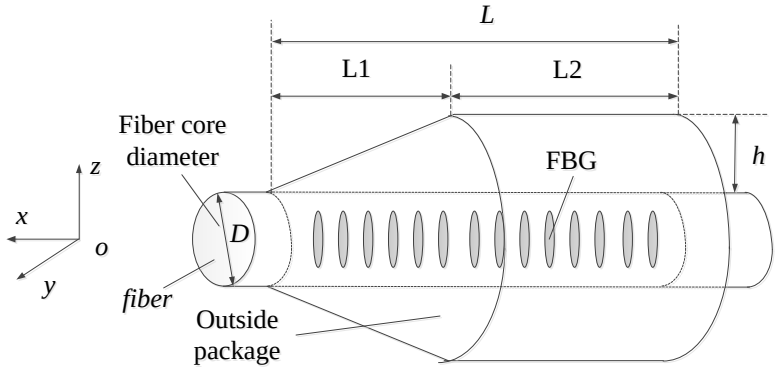

Fig.2 The packaging structure of the novel FBG probe

The FBG is wrapped with the same temperature-sensitive material. However, the front and rear packaging forms are different. Its structure is conical on one side (L1) and cylindrical on the other (L2). So the sensitivity of the structures on both sides to temperature is the same, but the sensitivity to strain is different. It can be seen that when temperature and strain exist at the same time, the cylindrical segment can obtain temperature data, while the conical segment can obtain strain data, and the cross-sensitivity between the two parameters can be offset by the differential processing between the two. According to the functional relationship between the degree of refractive index modulation and the Bragg wavelength, the temperature-wavelength offset function can be calculated, and the chirped FBG can provide broadband reflection spectrum information, then the values of the two sets of parameters can be solved

$$\alpha_f = \lambda^{-1}\frac{d\lambda}{dT}, \xi = n^{-1}\frac{dn}{dT}, \Delta T = \left(\alpha_f + \xi\right)^{-1} \cdot \frac{\Delta\lambda_{L'}}{\lambda_{L'}} \tag{1}$$

where n is the refractive index, ξ is the thermo-optic coefficient, and α_f is the thermal expansion coefficient.

For the chirped FBG [15], if the chirped coefficient is F, the grating size is L, and the corresponding position of the grating is z ($0<z<L$), the grating period can be expressed as

$$\Lambda_i(z) = \left[1 - \frac{F}{L}z\right]\Lambda_0(z) \tag{2}$$

On this basis, the strain distribution change caused by the new FBG shell is introduced, and the strain function in the z-axis direction can be obtained according to Hooke's law

$$\varepsilon = \frac{L^2 \cdot F}{\pi Eh\left[DL + hz\right] \cdot z} \tag{3}$$

Among them, L is the grating size, h is the uniform thickness position of the shell, D is the fiber diameter, F is the stress, E is the elastic modulus, and z is any point on the grating. It can be seen from the above formula that the stress and the z-axis position together determine the reflection spectrum data obtained by the system, so the system can realize the analysis of strains in different dimensions.

4. Simulation Analysis

In order to further verify the feasibility of FBG structure design, the functional relationship between wavelength, temperature and strain was verified respectively. First analyze the temperature, set n=1.4352, ξ=6.37×10^{-6}m/℃, α_f = 5.24×10^{-7}m/℃, then the functions of temperature, strain and wavelength offset are shown in Fig. 3.

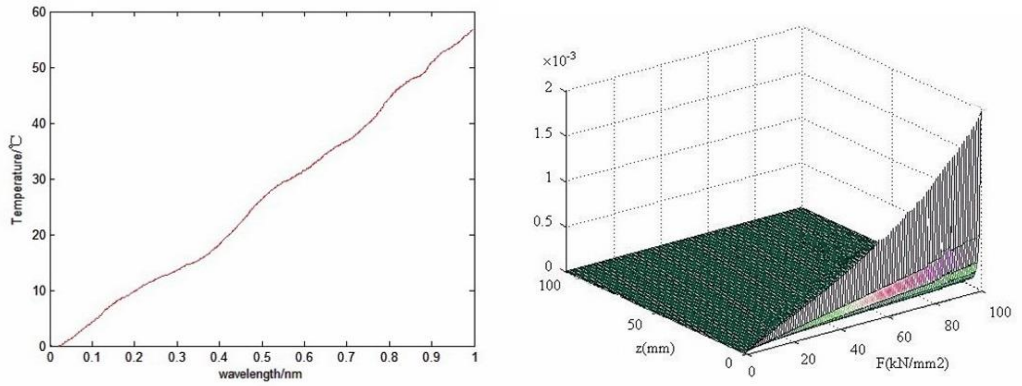

(a) Temperature as a function of wavelength (b) Strain as a function of wavelength

Fig.3 Two-parameter response function

It can be seen from Fig. 3(a) that when the echo light is offset, the change of temperature with wavelength is linear, and the wavelength change corresponding to 1.0°C is about 25.0pm. The wavelength and spectral distribution have completely different changes in strain. Let L=120mm, h=5.5mm, D=120□m, E=300kN/mm2, then the variation distribution is shown in Fig. 3(b). The test results show that the strain response caused by the FBG shape strain structure also has remarkable characteristics. In the fiber axis (z) direction, the spectral distribution change caused by strain is significantly different from the change caused by temperature, and this difference is also the key to the simultaneous analysis of the two parameters. With the increase of strain, the change effect is very obvious. It follows a linear relationship with the z-axis direction, and an exponential change with the F-direction. This change relationship is related to the wall thickness distribution of the outer structure.

5. Experiments

5.1 Temperature Calibration Test

The temperature test is completed with an adjustable temperature box, and the temperature test accuracy of the temperature box is ±0.5℃. The comparison test equipment uses the FOT2300 temperature detector to measure the same point, and the experimental results are shown in Fig. 4.

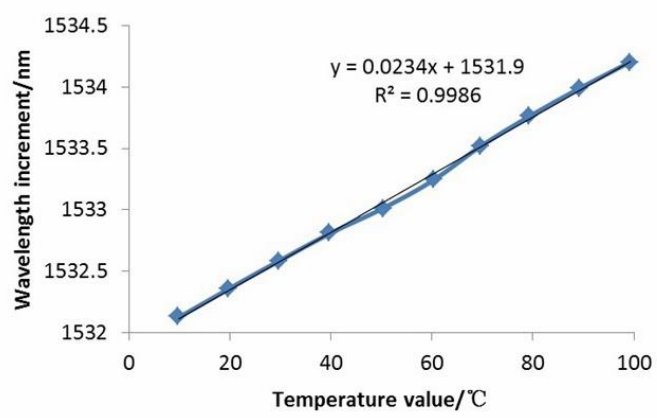

Fig.4 Temperature test curve

The temperature test value curve obtained by this system has a linearity of 0.9986, which can well reflect the change between temperature and wavelength. Compared with the FOT2300 temperature detector, the average relative error of its temperature test is about 1.3%, and it can be seen that the test effect meets the design requirements. The temperature test data based on optical fiber sensing is repeatable and stable in the test range of 10-100 °C. Its temperature measurement

performance is stable, and the error distribution of most of the data is around 0.68%. It can be seen that it is feasible to use this system to detect the temperature in real time.

5.2 Static Strain Test

After the temperature of the test system is calibrated, the stress state test can be completed. The test results below are all temperature corrected. The strain test process is mainly divided into two parts: static test and dynamic impact test, which respectively characterize the state response effect of the power device under static stress and dynamic stress.

In the static strain test, the pressure range is 0.1kN -1kN, and the stress field distribution of the transformer structure is inverted by analyzing the center wavelength offset. In the experiment, the center wavelength value was recorded once every 100N increase, and then the stress wavelength curve (×) was drawn; in the return test, the center wavelength value was recorded once every 100N decrease, and then the stress wavelength curve (+) was drawn, and the test results are shown in Fig. 5(a), in order to ensure that the system test range meets the design requirements, the test results from 1kN to 5kN are also completed, as shown in Fig. 5(b).

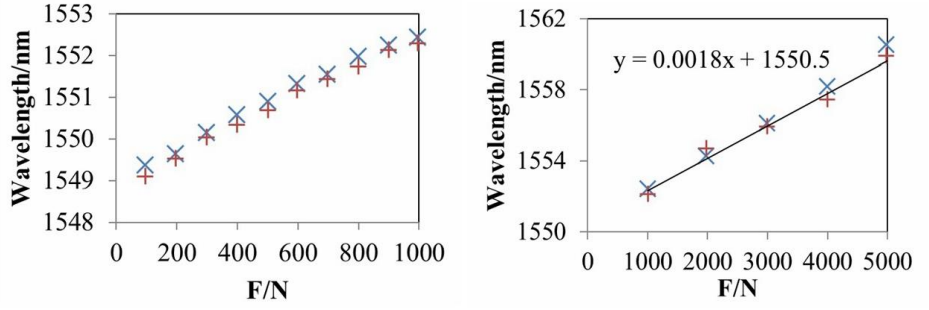

(a) 0.1kN-1kN (b) 1kN-5kN

Fig.5 Wavelength response curves of different stress ranges

The experimental results show that in different test intervals, the stress and wavelength can well satisfy the linear relationship, and the repeatability of the test results is verified by increasing and decreasing the applied force value. The fitting function of the wavelength shift with respect to the stress under different conditions calculated from the test data is as follows:

$$\begin{cases} y = 0.0036x + 1548.9 & 0.1kN < F < 1kN \\ y = 0.0018x + 1550.5 & 1kN < F < 5kN \end{cases} \tag{4}$$

It can be calculated according to the wavelength and stress range of the above formula. The test results of the first half show that the sensitivity of the system is 0.0036nm/N. The test results in the second half show that the system sensitivity is 0.0018nm/N. Since the wavelength resolution accuracy of the

demodulator in this system is 1pm, the system can accurately invert the stress field distribution at the position to be measured no matter which stress range it is in, which further verifies the feasibility of the system.

5.3 Dynamic Strain Test

Since the impact force generated by the free-falling heavy object hitting the sensor and the current impact coil is a pulse force, in the dynamic impact experiment, a 5kg heavy object was dropped from a height of 100mm, 200mm, 300mm and 40mm respectively to simulate dynamic impact. The center wavelength of the FBG in the sensor is shifted during the impact, and then the response capability and resolution accuracy of the dynamic impact of the system are calculated by analyzing the degree of wavelength shift. The test curves of four different heights are shown in Fig.6.

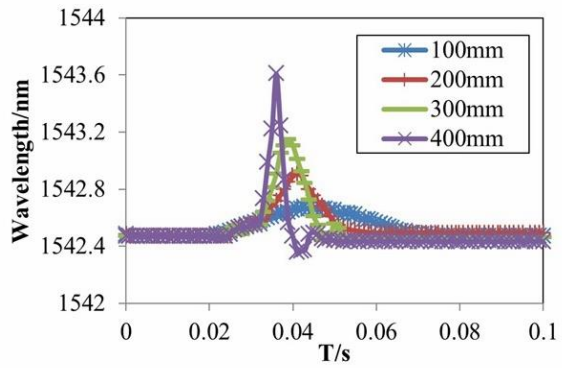

Fig.6 Wavelength response curves of different dynamic shocks

It can be seen from Fig. 6 that the wavelength response of the impact force caused by the falling object at different heights is different, and the wavelength shifts of the four positions are 0.2358nm, 0.4589nm, 0.7894nm and 1.1314nm respectively; the half-widths of the response times are 4.23ms, 3.14ms, 2.23ms and 1.09ms. The shock forces of the above four cases are calculated by the Torricelli equation to be 149.2N, 285.1N, 524.5N and 763.8N respectively. Combined with the wavelength offset obtained by the test, the average shock response sensitivity of the system can be fitted to be 0.00268nm/N. It can be seen from the response time that with the increase of the impact force, the response time continues to decrease. If the time-resolved method is used to complete the pulse force analysis, the sampling rate of the system is required to be better than 5.0kHz, so as to ensure that the details of the wavelength change with time can be was completely captured.

6. Conclusions

A state monitoring system for power devices based on optical fiber sensing is built. A dual-parameter response FBG sensor that simultaneously acquires temperature and stress is designed. Through the simulation calculation, the influence degree of different parameters on the wavelength response is analyzed. The temperature and static and dynamic strain were tested separately in the experiment, and the results show that the temperature drift has a good linearity and can be compensated by calibration. The static stress response curve also has high linearity and can be calculated from more than two sets of test data. The dynamic stress response curve can be calculated from the wavelength shift and the half-width of the response time. It provides a new idea for simultaneous monitoring and decoupling of multi-state parameters, which has a certain contribution to the application of rapid acquisition of power device states. However, this paper focuses on monitoring the state of simple structures in power devices and is not universal for special shapes or special locations. In future research, some special structural power devices will be tested and analyzed to improve the universality of the system.

Acknowledgement

This work was supported by Shanxi Provincial Applied Basic Research Project No.201701D221124, Shanxi Provincial Key R & D Project No.201903D221025.

R E F E R E N C E S

[1]. *LU Ping, LALAM N, BADAR M, et al.,* "Distributed optical fiber sensing: Review and perspective", Applied Physics Reviews, **vol. 6,** no. 4, 2019, pp.041302.

[2]. *Boujia N., Schmidt F., Chevalier C.,* "Distributed optical fiber-based approach for soil-structure interaction", Sensors, **vol. 20,** no.1,2020, pp. 1-14.

[3]. *B. Yang, X. Li, Y. Hou, A. Meier, X. Cheng, J. H. Choi,* "Non-invasive (non-contact) measurements of human thermal physiology signals and thermal comfort/discomfort poses - A review", Energy and Buildings, **vol. 224,** no. 1, 2020, pp.110261.

[4]. *Liu Yunpeng, Tian Yuan, Fan Xiaozhou, et al.,* "Detection and identification of transformer winding strain based on distributed optical fiber sensing", Applied Optics, **vol. 57,** no. 22, 2018, pp: 6430-6438.

[5]. *HAMMON T E, STOKES A D.,* "Optical fiber Bragg grating temperature sensor measurements in an electrical power transformer using a temperature compensated optical fiber Bragg grating as a reference", Proceedings of 11th International Conference on Optical Fiber Sensors. Sapporo, Japan: OSA, 1996, pp.566-569.

[6]. *YI Jiang, LIU Shuang, LI Xiao, et al.,* "Fiber Bragg grating sensors for temperature monitoring in oil-immersed transformers", International Conference on Optical Communications and Networks. Hangzhou, China: IEEE, 2016, pp.1-3.

[7]. *WICKERSHEIM K A.,* "Optical temperature measurement technique utilizing phosphors", US4215275, 1980-07-29.

[8]. *ZHAO Yong, CHEN Maoqing, LÜ Riqing, et al.*, "Small and practical optical fiber fluorescence temperature sensor", IEEE Transactions on Instrumentation and Measurement, **vol. 65,** no. 10, 2016, pp. 2406-2411.
[9]. *ZHAO Yongtan, PANG Chenlei, WEN Zhong, et al.*, "A microfiber temperature sensor based on fluorescence lifetime", Optics Communications, **vol. 426,** no. 6, 2018, pp. 231-236.
[10]. *LU Lidong, YUN Liang, LI Binglin, et al.*, "Experimental study on location of lightning stroke on OPGW by means of a distributed optical fiber temperature sensor", Optics and Laser Technology, **vol. 65,** no. 1, 2015, pp. 79-82.
[11]. *ZHAO Long, HUANG Xinbo.*, "Integrated condition monitoring system of transmission lines based on fiber Bragg grating sensor", 2016 International Conference on Condition Monitoring and Diagnosis. Xi'an, China: IEEE, 2016, pp. 667-670.
[12]. *MA Guoming, LI Yabo, MAO Naiqing, et al.*, "A fiber Bragg grating-based dynamic tension detection system for overhead transmission line galloping", Sensors, **vol. 18,** no. 2, 2018, pp.365-370.
[13]. *WYDRA M, KISALA P, HARASIM D, et al.*, "Overhead transmission line sag estimation using a simple optomechanical system with chirped fiber Bragg gratings. Part 1: Preliminary measurements", Sensors, **vol.18,** no. 1, 2018, pp. 309-312..
[14]. *Leal Junior Arnaldo G., Theodosiou Antreas, Marques Carlos, et al.*, "Compensation Method for Temperature Cross-Sensitivity in Transverse Force Applications With FBG Sensors in POFs", Journal of Lightwave Technology, **vol. 36,** no. 17, 2018, pp. 3660-3665.
[15]. *J. Yan, Y. Meng, X. Yang, X Luo*, "Privacy-Preserving localization for underwater sensor networks via deep reinforcement learning", IEEE Transactions on Information Forensics and Security, **vol. 1,** no. 99, 2020, pp. 1–12.